Int. J. Oral Maxillofac. Surg. 2019; 48: 971–981
https://doi.org/10.1016/j.ijom.2018.12.009, available online at https://www.sciencedirect.com

International Journal of Oral & Maxillofacial Surgery

Research Paper
Dental Implants

Evaluation of the surface damage of dental implants caused by different surgical protocols: an in vitro study

P. Streckbein[1], J.-F. Wilbrand[1], C. Kähling[1], J. Pons-Kühnemann[2], P. Rehmann[3], B. Wöstmann[3], H.-P. Howaldt[1], S. C. Möhlhenrich[4]

[1]Department of Cranio-Maxillo-Facial Surgery, University Hospital, Justus-Liebig-University, Gießen, Germany; [2]Department of Medical Statistics, Justus-Liebig-University, Gießen, Germany; [3]Department of Prosthetic Dentistry, University Hospital, Justus-Liebig-University, Gießen, Germany; [4]Department of Orthodontics and Dentofacial Orthopaedics, University Hospital of RWTH Aachen, Aachen, Germany

P. Streckbein, J.-F. Wilbrand, C. Kähling, J. Pons-Kühnemann, P. Rehmann, B. Wöstmann, H.-P. Howaldt, S.C. Möhlhenrich: Evaluation of the surface damage of dental implants caused by different surgical protocols: an in vitro study. Int. J. Oral Maxillofac. Surg. 2019; 48: 971–981.

Abstract. The implant surface must withstand high insertion torque during implant insertion. The aim of this study was to investigate the damage to implant surfaces caused by two different insertion protocols in vitro. Fifteen titanium implants per group were inserted in standardized polyurethane foam models, group 1 according to a non-threaded surgical protocol and group 2 according to a threaded surgical protocol. Before and after insertion, the surfaces were visualized by scanning electron microscopy (SEM) and non-contact laser profilometry. Different surface area parameters were evaluated and maximum torque during insertion was determined. SEM detected topographical changes such as deposition of the test block and smoothening of the surface in the region of the thread crests in both groups. The laser profilometry analysis revealed significant changes in the surface topography of the implants in both groups, but no differences between the groups. Insertion torque was significantly decreased in the threaded group. Both types of surgical intervention resulted in surface damage. Less damage was detected to the thread crests with the use of a thread cutter, and most of the surface was not visibly affected by the surgical protocol at the microscopic level. The surgical protocol seems to have a minor influence on preservation of the implant surface.

Key words: dental implant; implant surface; surface characterization; surface damage; insertion torque; laser profilometry.

Accepted for publication 13 December 2018
Available online 26 January 2019

Osseointegration and mechanical long-term stability are prerequisites for a successful outcome in dental implantology[1]. Various reports have demonstrated increased bone–implant contact rates and improved osseointegration due to modifications of the implant surface[2–6]. However, numerous studies have reported the presence of loose titanium particles in the bone around smooth-turned grit-blasted/acid-etched and plasma-sprayed implants[7–11]. Additionally, soft tissue biopsies obtained from patients 6 months after implant installation were shown to contain titanium

particles in the connective tissue facing the dental implants[12].

Investigations have been published on changes to implant surfaces following insertion[13–15]. David[13] examined the surfaces of different implant systems after insertion using scanning electron microscopy (SEM) and was able to detect significant changes. These were described as grooves and abraded facets. Mints et al.[14] examined the surface integrity associated with implant placement. They studied common types of dental implant surfaces and evaluated how they were affected by the insertion procedure into polyurethane blocks. Comparisons between implants before and after insertion were made by SEM and roughness interferometry. They reported the presence of surface damage after the insertion of experimental anodized implants associated with loose titanium particles at the interface. Furthermore, Senna et al.[15] also quantified the surface damage caused by the insertion procedure of dental implants by means of roughness parameters, and investigated the presence of loose particles in the bone contact area. They concluded that shearing forces during insertion alter the dental implant surfaces and lead to metal particles in the surrounding bone, especially around surfaces composed mainly of peaks and with increased height parameters. In this context, Bartold et al.[16] investigated bone tissue that was damaged by implant insertion and found that insertion of a rough cylindrical implant type resulted in an increased fraction of micro-damaged bone matrix in comparison to rough tapered, smooth cylindrical, and smooth tapered implants. Depending on the quality of bone and the number of cracks present, this could lead to osteolysis in the bone tissue and reduced stability, explained by the fact that implant surfaces must withstand up to 50 N cm insertion torque during insertion[17]. The magnitude of these forces depends on differences in the surgical insertion protocols. In non-threaded interventions, the implant is inserted in a self-cutting manner. In threaded interventions, a thread cut is performed prior to implant installation.

No systematic evaluation of the influence of the surgical insertion protocol on the surface microstructure has been performed to date. The aim of this study was to determine the quantitative and qualitative extent of the damage to the surface of dental implants caused by two different surgical insertion protocols in vitro, in order to decrease the surface damage of dental implants and achieve the best possible conditions for osseointegration.

Materials and methods

Thirty uniform rotation symmetric tapered dental implants (BEGO Semados RI; diameter: 4.1 mm; length: 13 mm; BEGO GmbH & Co. KG, Bremen, Germany) were divided into two groups. Group 1 implants ($n = 15$) were used in a non-threaded insertion protocol and group 2 implants ($n = 15$) in a threaded insertion protocol. The implants were manufactured from grade 4 pure titanium with an acid-etched and sand-blasted surface ($R_a = 2.5$), a total surface area of 2.26 cm^2, and a thread crest length of 7.5 cm. The titanium properties of the implants are in accordance with ASTM F67-13, with tensile strength of 550 MPa and yield strength of 483 MPa. The difference between the two intervention groups was the use of a thread cutter prior to implant installation (Fig. 1).

The implants were inserted into homogeneous, biomechanically rigid foam blocks with a density of 30 PCF (solid rigid polyurethane foam; Sawbones, Malmö, Sweden). These grade 30 polyurethane foam blocks conform with the guidelines of ASTM International, with a compressive strength of 18 MPa and a compressive modulus of 445 MPa. These standard artificial bone blocks are well accepted for biomechanical examinations, as well as for measuring heat generation and drill wear during dental implant site preparation[18].

Multiple reference points on the implant surface were defined as regions of interest (ROIs); these included the second, eighth, and fourteenth thread flanks (ROIs 1–3) (Fig. 2). These ROIs were examined by SEM (LEO 982 Digital Scanning Microscope; Carl Zeiss, Inc., Thornwood, NY, USA) before and after insertion. Additionally, ROIs 1–3 were assessed using a laser profilometer before and after insertion (FRT MicroProf 100; FRT GmbH, Bergisch Gladbach, Germany) (Fig. 3). Due to the significant damage and the considerable polyurethane residues, the thread crests were also examined by SEM after implant removal (ROIs 4–6). However, an investigation by profilometry was not possible due to the curvature of the thread crests.

Implant insertion and removal

All implants were inserted following the two surgical protocols and as recommended by the manufacturer. The drilling was performed using a standardized box column drill (Gebr. Brasseler, Lemgo, Germany) controlled by DASYLab software (version

Fig. 1. The thread-cutter used in the threaded surgical protocol. The use or not of this cutter represents the difference in the surgical protocols between the tested groups.

Fig. 2. Tested dental implant. ROIs 1–3 represent the thread flanks and ROIs 4–6 represent the thread crests. Laser profilometry was performed for ROI 1–3 before and after insertion. SEM images were obtained before insertion at ROIs 1–3 and after insertion at ROIs 1–6.

10.00.01; National Instruments, Austin, TX, USA). Consistent drilling parameters were applied (depth 13.5 mm, 800 rpm, feed 0.5 mm/min).

For the thread cutting (group 2) and implant insertion (groups 1 and 2), an implant engine with a contra-angle was used (transmission 27:1; KaVo Dental GmbH, Biberach an der Riß, Germany). The thread cutter and implants were inserted at 25 rpm. During insertion of the implants, the maximum torque was registered with the standard box column drill (DMS; Gebr. Brasseler, Lemgo, Germany).

Following insertion, all implants were removed from the test blocks in a counter-clockwise direction and cleaned in an ultrasound bath (Bandelin Sonorex, Berlin, Germany). To remove polyurethane residues, the implants were placed into an acetone bath for 10 days, as recommended by the manufacturer (Sawbones, Malmö, Sweden).

Analysis of the surface area by SEM

The evaluation of the thread flanks (ROIs 1–3) by SEM was performed at 100-, 1000-, and 10,000-fold magnification at an operating distance of 20 mm and an acceleration voltage of 5 kV (per ROI and magnification: $n = 15$). The 100-fold magnification visualized an area of 1×1 mm, the 1000-fold magnification an area of 100×100 µm, and the 10,000-fold magnification an area of 10×10 µm. Supplementary images of the thread crests were prepared following insertion (ROIs 4–6). The resolution of all generated images was 1024×1024 pixels, and a descriptive analysis was performed.

Analysis of the surface area by laser profilometer

The surface structure was determined at each ROI (0.25 mm × 0.25 mm) using a laser profilometer (FRT GmbH, Bergisch Gladbach, Germany). FRT Mark III software (version 3.9) was used for topographic analyses. Alignment in a three-dimensional coordinate system using FRT Acquire software enabled exact repositioning of the measuring position before and after insertion.

A cut-off length of 35.74 µm, amplitude transmission with a cut-off wavelength of 50%, and application of a Gaussian filter were used for the analysis of all parameters. The surface area topography was characterized by: (1) amplitude parameters: S_a = average height deviation, S_{sk} = skewness (degree of symmetry of the surface heights about the

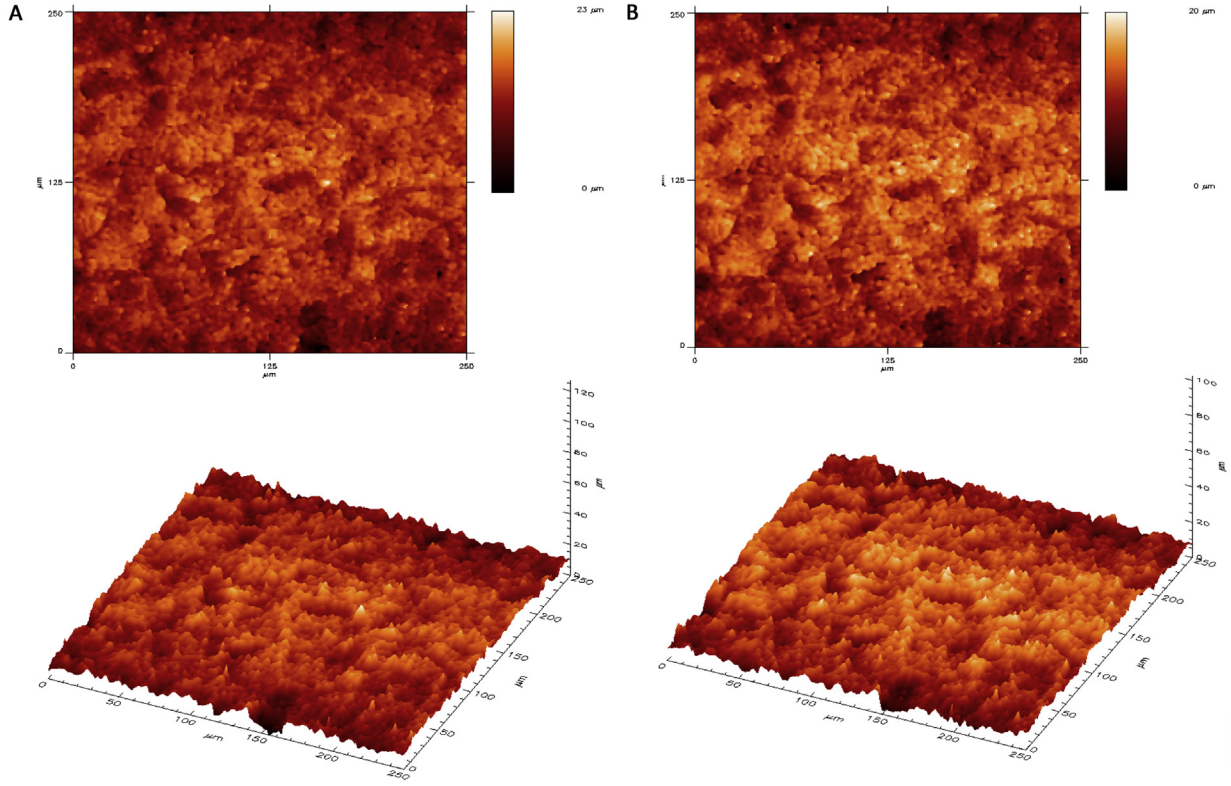

Fig. 3. Surface topography of an implant thread (BEGO Semados RI; BEGO Implant Systems, Bremen, Germany) by laser profilometry (A) before and (B) after insertion into artificial polyurethane bone blocks.

mean plane); (2) hybrid parameters: S_{dr} = developed interfacial area ratio, S_{3A} = surface area taking the vertical height into account; (3) functional parameters: S_{vk} = valley depth below the core roughness, S_k = core roughness height of the surface with the predominant peaks and valleys removed, S_{pk} = peak height above the core roughness; and (4) peak density: S_{pd} = number of peaks per unit area.

Statistical analysis

Data were recorded as the mean ± standard deviation values. The data normality was proved using the Kolmogorov–Smirnov test. Surface analysis data were submitted to two-way repeated-measures general linear model (GLM), and Bonferroni adjustment was applied within each analysis. The statistical analysis of insertion torque was performed by Mann–Whitney *U*-test.

Results

SEM prior to insertion

Evaluation of the ROI on the SEM images at 100×, 1000×, and 10,000× magnification revealed no deviations in surface area topography for each implant within or among the test groups (Fig. 4).

SEM following insertion

Despite the manufacturer's prediction, a 10-day acetone bath did not completely remove the polyurethane residues.

At 100× magnification, there were no changes in the surface area structures of the flanks (ROIs 1–3), but deposition of polyurethane test specimen (up to 200 μm) was observed on the crest threads (ROIs 4–6) in both groups (Fig. 5). Differences were found in the distribution and quantity of polyurethane residues between the two groups. Compared to the non-threaded insertion group (group 1), the threaded insertion group (group 2) showed more

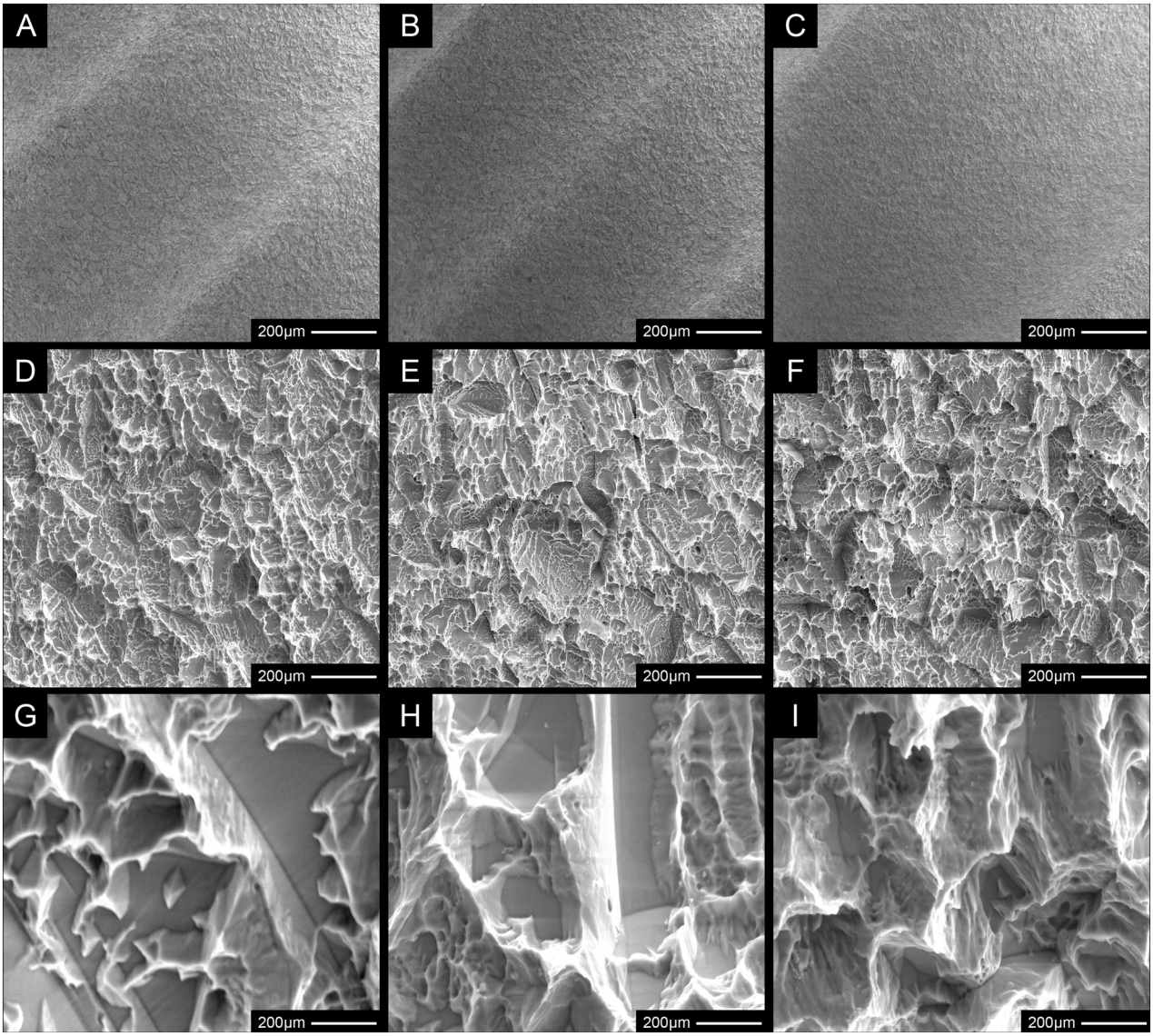

Fig. 4. Implant before insertion at 100× magnification. (A) ROI 1, (B) ROI 2, (C) ROI 3. Implant before insertion at 1000× magnification. (D) ROI 1, (E) ROI 2, (F) ROI 3. Implant before insertion at 10,000× magnification. (G) ROI 1, (H) ROI 2, (I) ROI 3.

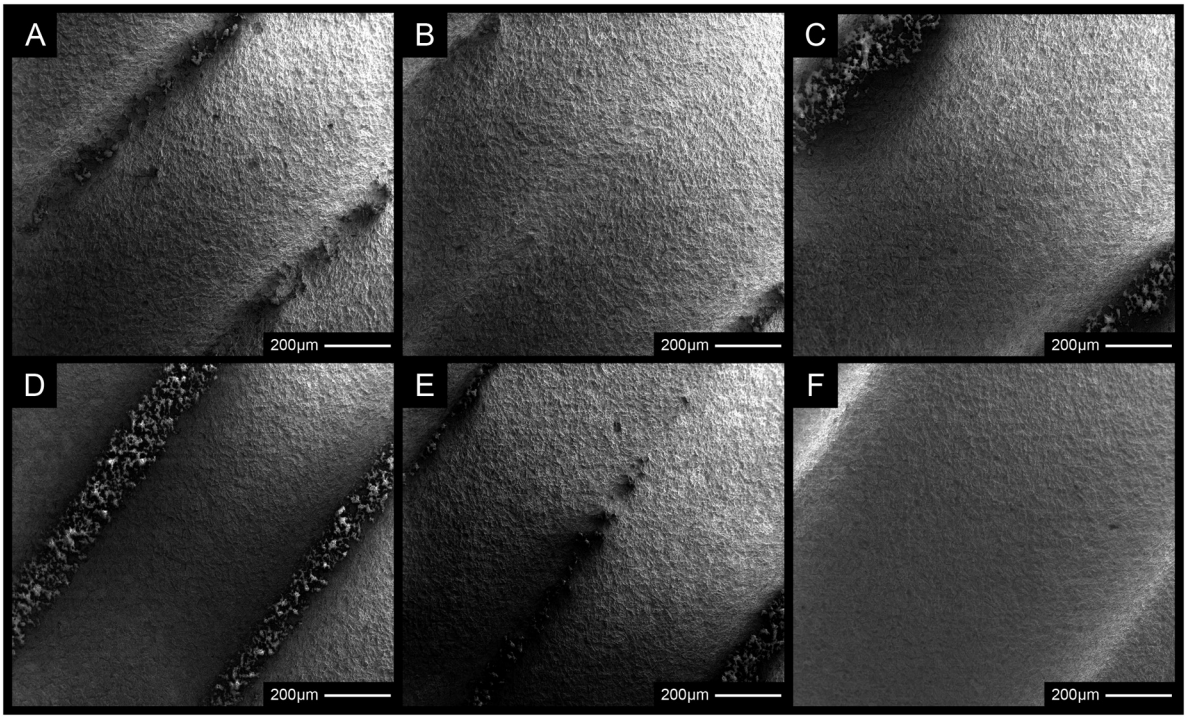

Fig. 5. Implant thread flanks and crests after insertion, at 100× magnification: (A–C) non-threaded protocol; (D–F) threaded protocol.

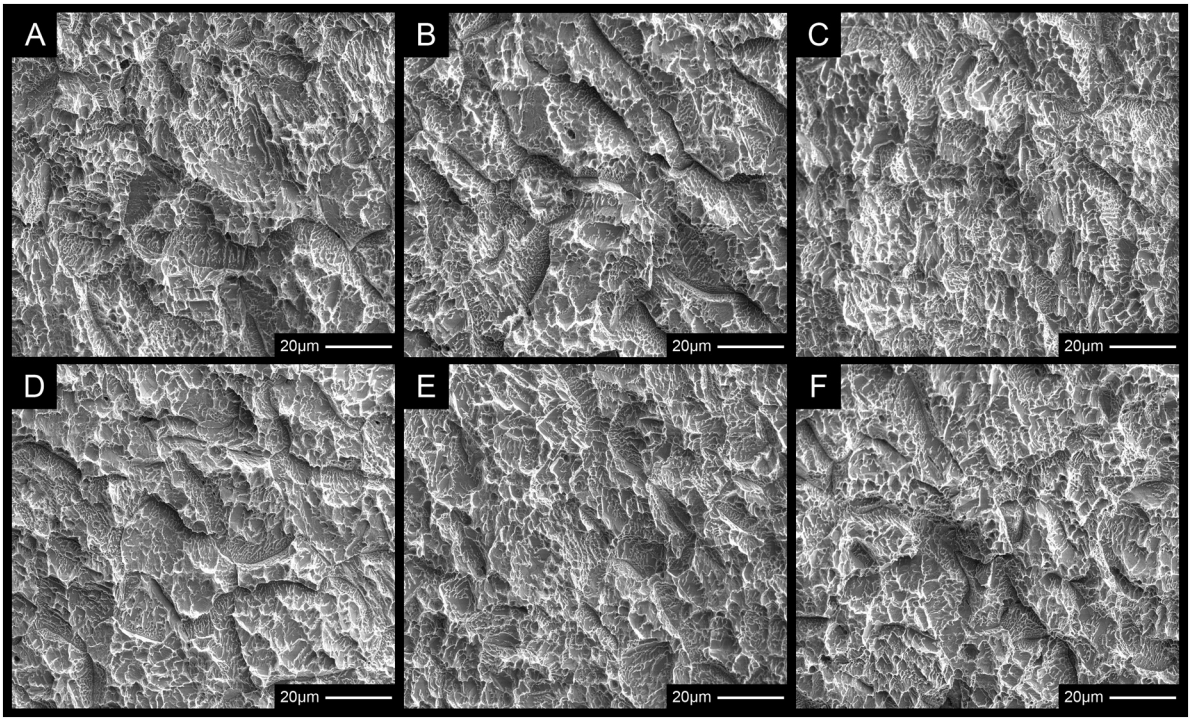

Fig. 6. Implant thread flanks after insertion at 1000× magnification, non-threaded protocol: (A) ROI 1, (B) ROI 2, (C) ROI 3. Implant thread flanks after insertion at 1000× magnification, threaded protocol: (D) ROI 1, (E) ROI 2, (F) ROI 3.

residues at the crestal threads and less at the implant tip.

Examination at 1000× magnification revealed no visible changes in the surface area structures of the flanks (ROIs 1–3) (Fig. 6). In contrast, topographical differences such as surface levelling and abrasion facets were noted on the thread crests (Fig. 7). The distribution of polyurethane residues in the two groups was analogous to that seen at 100× magnification.

SEM at 10,000× magnification also demonstrated no structural changes to the surface areas of the flanks (ROIs

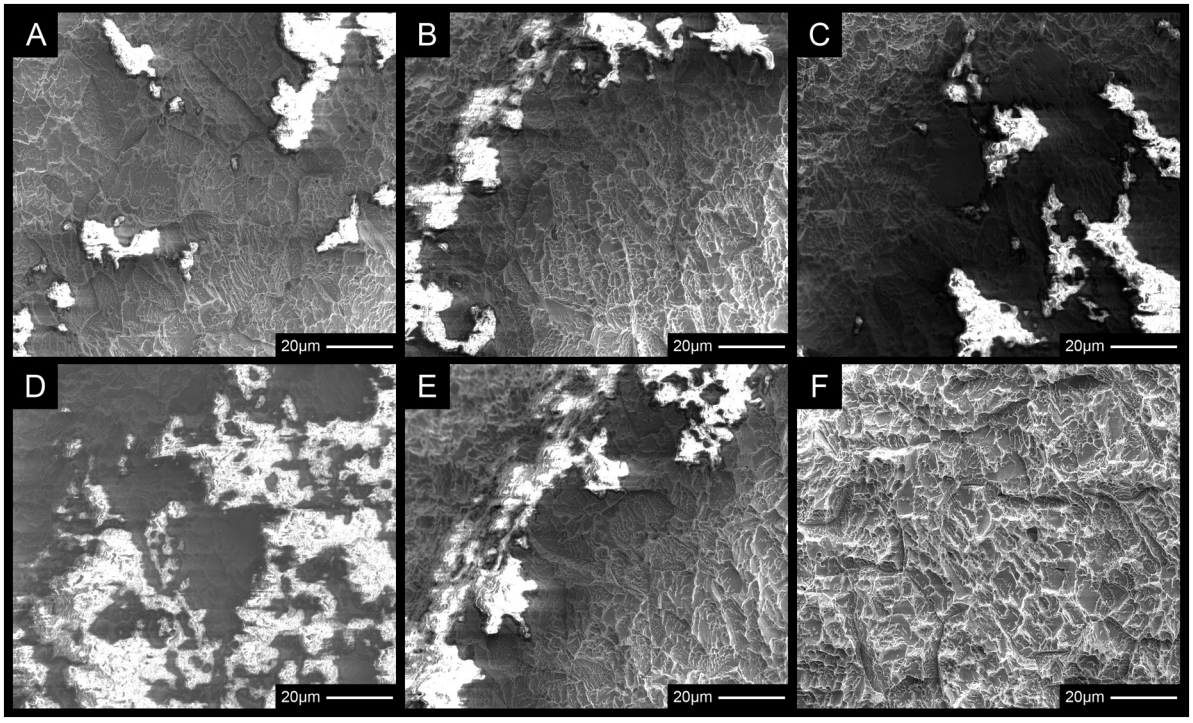

Fig. 7. Implant thread crests after insertion at 1000× magnification, non-threaded protocol: (A) ROI 4, (B) ROI 5, (C) ROI 6. Implant thread crests after insertion at 1000× magnification, threaded protocol: (D) ROI 4, (E) ROI 5, (F) ROI 6.

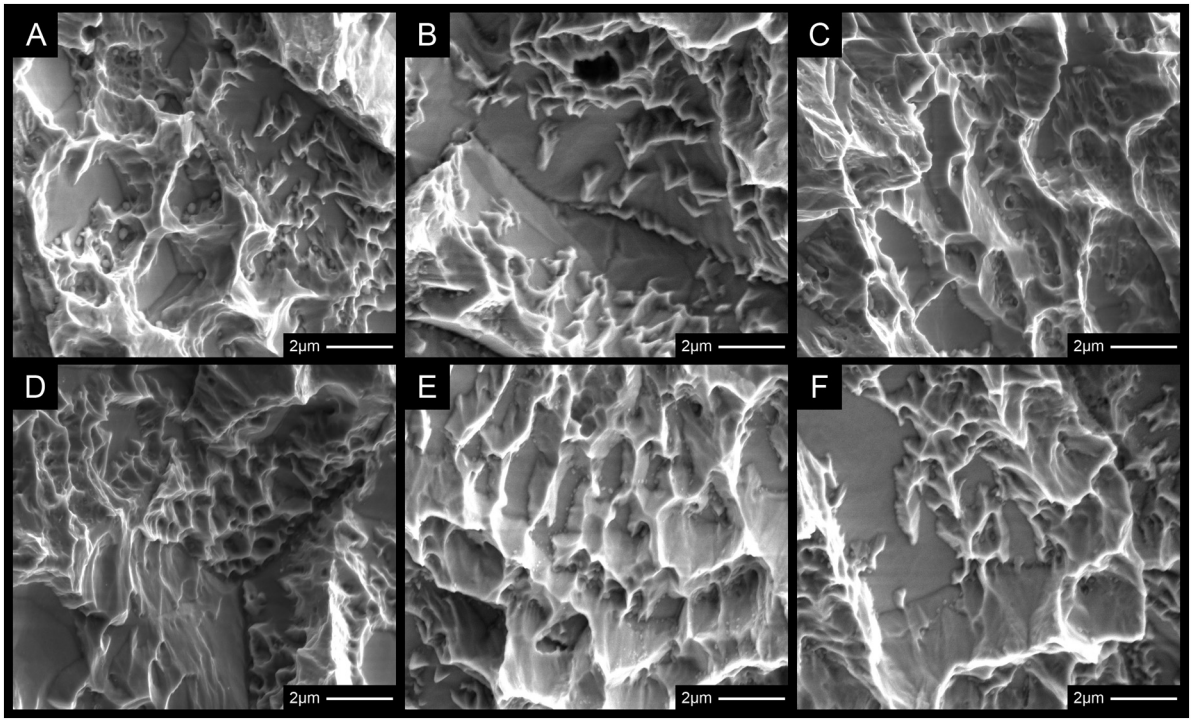

Fig. 8. Implant thread flanks after insertion at 10,000× magnification, non-threaded protocol: (A) ROI 1, (B) ROI 2, (C) ROI 3. Implant thread flanks after insertion at 10,000× magnification, threaded protocol: (D) ROI 1, (E) ROI 2, (F) ROI 3.

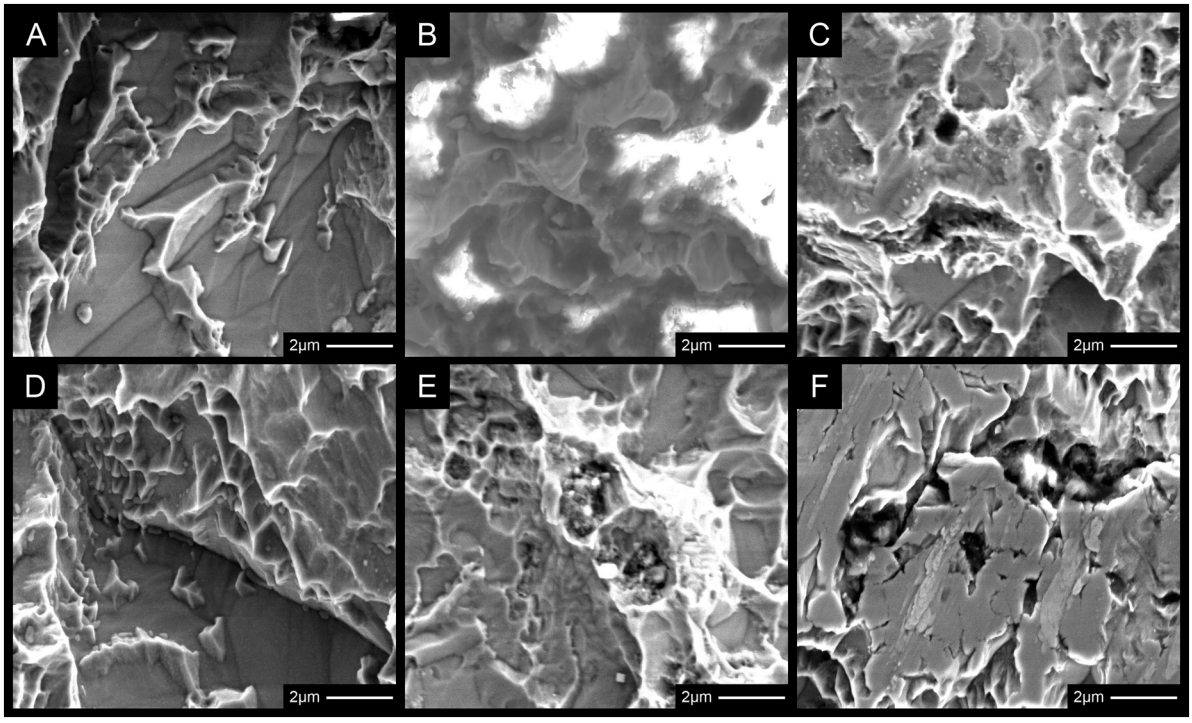

Fig. 9. Implant thread crests after insertion at 10,000× magnification, non-threaded protocol: (A) ROI 4, (B) ROI 5, (C) ROI 6. Implant thread crests after insertion at 10,000× magnification, threaded protocol: (D) ROI 4, (E) ROI 5, (F) ROI 6.

1–3) (Fig. 8). Besides intact surface area topographies (Fig. 9A, D), polyurethane depositions, porous deposits (Fig. 9B, E), abrasion facets, and surface levelling (Fig. 9C, F) were noted at the crests.

Laser profilometer

Outcomes and comparisons of the average values for the surface parameters (S_a, S_{sk}, S_{dr}, S_{3A}, S_{vk}, S_k, $S_{pk,and}$ S_{pd}) are shown in Figs 10–13.

Laser profilometry analysis of the flank surface topography prior to and following implant insertion revealed significant differences in both groups (group 1, non-threaded; group 2, threaded). These differences oc-

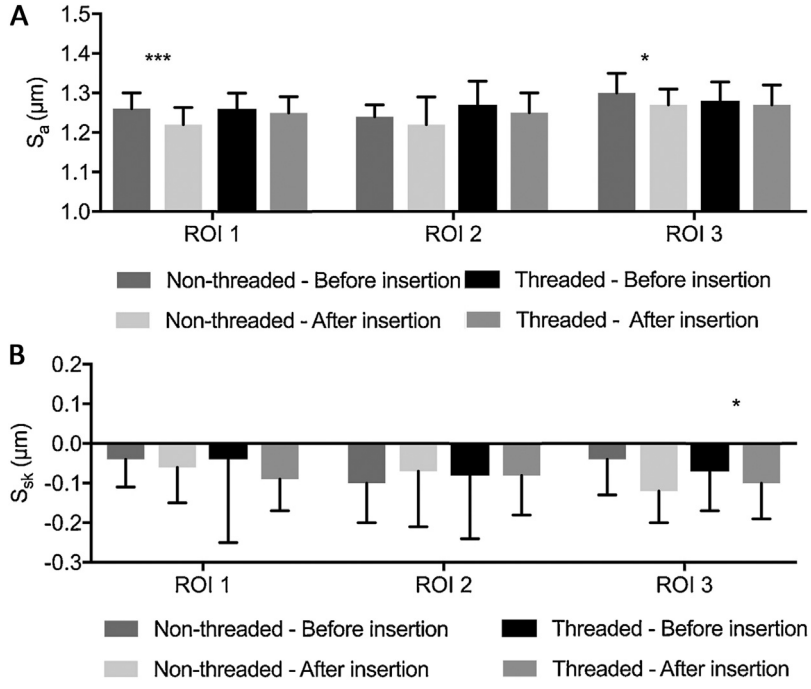

Fig. 10. Surface roughness of the amplitude parameters: (A) S_a and (B) S_{sk} of the implants before and after insertion into bone depending on the surgical protocol: threaded vs. non-threaded (*$P \leq 0.05$, **$P \leq 0.01$, and ***$P \leq 0.001$) (S_a = average height deviation; S_{sk} = degree of symmetry of the surface heights about the mean plane).

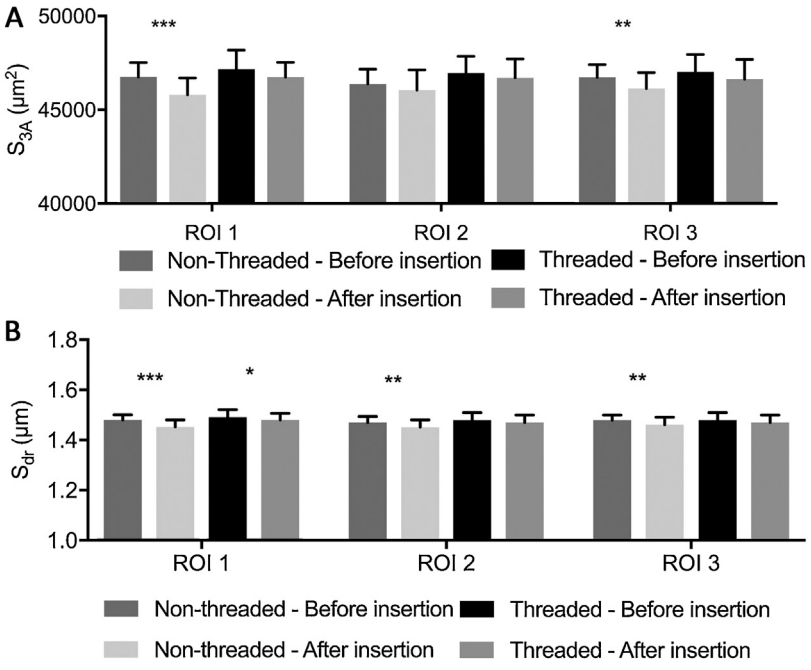

Fig. 11. Surface roughness of the hybrid parameters: (A) S_{3A} and (B) S_{dr} of the implants before and after insertion into bone depending on the surgical protocol: threaded vs. non-threaded (*$P \leq 0.05$, **$P \leq 0.01$, and ***$P \leq 0.001$) (S_{dr} = developed interfacial area ratio, S_{3A} = surface area taking the vertical height into account).

curred predominantly at ROIs 1 and 3 in group 1 (non-threaded) after the intervention. The comparison of the different surgical protocols (non-threaded vs. threaded) showed no significant differences.

Alterations of the arithmetic mean height (S_a) were observed in the non-threaded protocol (group 1) (Fig. 10A). The S_a decreased significantly after implant insertion in two ROIs (ROI 1: 1.26 ± 0.04 µm to 1.22 ± 0.04 µm, $P = 0.001$; ROI 3: 1.30 ± 0.05 µm to 1.27 ± 0.04 µm, $P = 0.05$). Regarding the skewness (S_{sk}), a significant difference was found only in ROI 3 after the threaded protocol: -0.07 ± 0.10 µm to -0.10 ± 0.09 µm, $P = 0.048$ (Fig. 10B).

The hybrid parameters in group 1 (non-threaded protocol) indicated a marked change in surface area topography. Significant changes were noted in the actual surface area S_{3A} (ROI 1: $46{,}764.508 \pm 771.986$ µm² to $45{,}806.937 \pm 899.847$ µm², $P < 0.001$; ROI 3: $46{,}743.069 \pm 667.493$ µm² to $46{,}155.009 \pm 840.409$ µm², $P = 0.0011$) (Fig. 11A). In contrast, no significant decrease in this parameter was identified in group 2 (threaded protocol). The developed interfacial area ratio (S_{dr}) showed

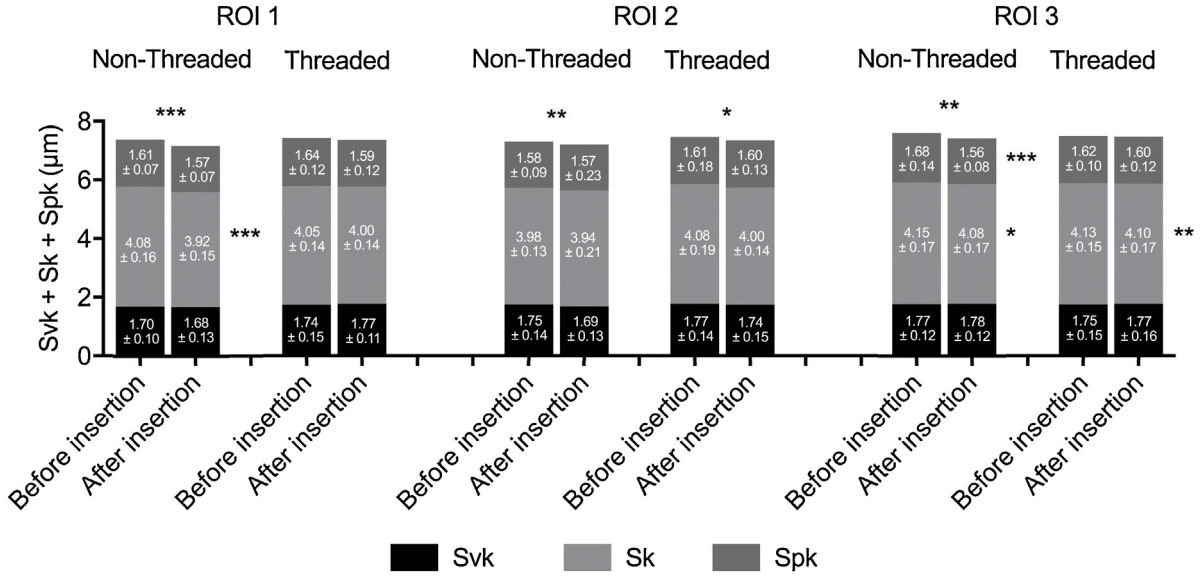

Fig. 12. Surface roughness of the functional parameters: S_{vk}, S_k, and S_{pk} of the implants before and after insertion into bone depending on the surgical protocol: threaded vs. non-threaded (*$P \leq 0.05$, **$P \leq 0.01$, and ***$P \leq 0.001$) (S_{vk} = valley depth below the core roughness; S_k = core roughness height of the surface with the predominant peaks and valleys removed; S_{pk} = peak height above the core roughness).

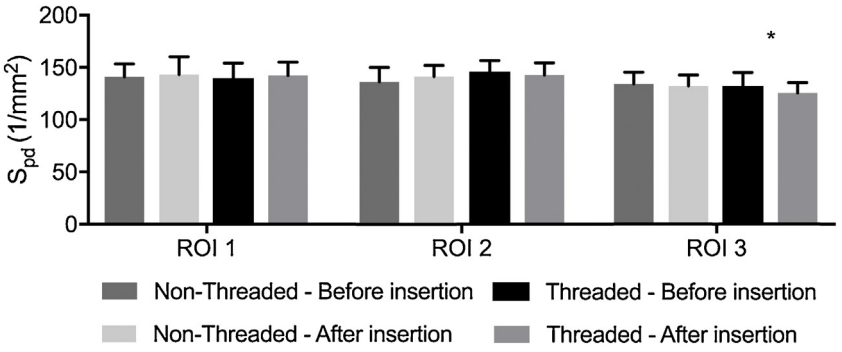

Fig. 13. Peak density of the implants before and after insertion into bone depending on the surgical protocol: threaded vs. non-threaded (*$P \leq 0.05$, **$P \leq 0.01$, and ***$P \leq 0.001$) (S_{pd} = number of peaks per unit area).

significant changes at all three measurement positions in group 1 (ROI 1: 1.48 ± 0.02 μm to 1.45 ± 0.03 μm, $P < 0.001$; ROI 2: 1.47 ± 0.02 μm to 1.45 ± 0.03 μm, $P = 0.005$; ROI 3: 1.48 ± 0.02 μm to 1.46 ± 0.03 μm, $P = 0.005$) (Fig. 11B). In group 2, S_{dr} decreased significantly from 1.49 ± 0.03 μm to 1.48 ± 0.03 μm in ROI 1 ($P = 0.035$).

In terms of the surface functional height parameters, the core roughness depth (S_k) showed significant changes in group 1: ROI 1 4.08 ± 0.16 μm to 3.92 ± 0.15 μm ($P < 0.001$) and ROI 3 4.15 ± 0.17 μm to 4.08 ± 0.17 μm ($P = 0.041$). Additionally, surface alterations were also detected in group 2 in ROI 3: 4.13 ± 0.15 μm to 4.10 ± 0.17 μm ($P = 0.012$) (Fig. 12). Furthermore there was a significant decrease in peak height above the core roughness (S_{pk}) from 1.68 ± 0.14 μm to 1.56 ± 0.08 μm ($P = 0.002$) in ROI 3 in group 1. The valley depth below the core roughness (S_{vk}) showed no changes in either group.

Regarding peak density (S_{pd}), a significant decrease from 132 ± 12.81 peaks/mm^2 to 124.4 ± 9.72 peaks/mm^2 was only found in ROI 3 in group 2 ($P = 0.044$) (Fig. 13).

Insertion torque

The maximum insertion torque was 52.62 ± 7.59 N cm in group 1 and 28.24 ± 18.38 N cm in group 2. Thread cutting (group 2) led to a significant decrease in insertion torque ($P = 0.019$).

Discussion

Numerous modifications have been made to dental implants. A number of investigations of nano-modifications to the implant surface have been published recently[19–22]. Several approaches involving micro-modification of the surface of implants to improve osseointegration have been described[23,24]. Roughening modifications such as acid-etching and/or sand-blasting have been used clinically[2,15]. Published studies have investigated the effect of surface modifications on osseointegration. Roughened surfaces have been found to be associated with a significantly increased bone–implant contact rate compared with machined surfaces[25–27].

Different ex vivo models like cow ribs or pig pelvic bone exist for the simulation of a human maxilla and mandible. However, the cortical thickness varies, e.g. in pig pelvic bone, the thickness is between approximately 0.5 mm and 2.5 mm[28]. This affects the primary stability[29] and possibly also the loading of the implant surface during insertion. Therefore, polyurethane blocks were used to achieve the highest possible standardization. These blocks are widely used for mechanical testing of dental implants[18,30–32]. Previous results have suggested that grade 30 polyurethane blocks are similar to bone type 3 or 4[33]. Although these polyurethane blocks are softer than titanium, Mints et al.[14] were able to demonstrate that the insertion of implants into this material, with a density of 30 PCF, leads to implant surface damage. This may be due to the surface modification, which results in a surface that is more porous compared to machined surfaces.

Abrasion of titanium particles during insertion and their enclosure in peripheral tissues such as cervical lymph nodes has been reported[34,35]. The loss of titanium particles means that the surface must have been damaged during the implant insertion. Both Mints et al.[14] and Senna et al.[15] investigated changes in implant surfaces following insertion. Mints et al.[14] reported that anodized implants in particular demonstrated extensive damage associated with insertion; e.g., the entire porous oxide layer was removed in the apical region and on the crests of the threads, and the roughness parameters S_p and S_{pk} were increasingly reduced. Furthermore, the polyurethane foam blocks in contact with the anodized implants demonstrated loose titanium particles. Senna et al.[15] investigated three different implants representing different surface topographies after insertion in fresh cow rib bone blocks by SEM and interferometry. They reported that amplitude and hybrid roughness parameters of all three groups were lower after insertion and that the surfaces presenting a predominance of peaks (S_{sk} (skewness) > 0) associated with higher structures presented higher damage associated with a more pronounced reduction of material volume. Additionally, the SEM images demonstrated loose titanium and aluminium particles at the interface, mainly at the crestal cortical bone level. Therefore, they concluded that shearing forces during the insertion procedure alter the implant.

To date, no systematic evaluation of the effect of different surgical protocols on implant surface microstructure damage has been implemented. In the present study, a commercially available implant with an acid-etched and sand-blasted surface was investigated to determine the quantitative and qualitative extent of the surface damage caused by two different surgical insertion protocols (non-threaded vs. threaded). Assessments were conducted according to the guidelines for topographic evaluation of implant surfaces[36]. Roughness parameters used for the characterization of implant surfaces are subdivided into amplitude, spatial, and hybrid parameters. The three-dimensional implant geometry itself and remaining residues of the biomechanical test block (polyurethane) after implant insertion restricted the investigation of thread crests by means of SEM and laser profilometry. Despite the manufacturer's

recommendations, a 10-day acetone bath did not completely remove the polyurethane residue.

The results of this study showed that the use of a thread cutter significantly decreased insertion torque and resulted in decreased stress to the implant surface, as indicated by abrasion facets, surface levelling, and increased polyurethane residues. The excessive compressive strength and shear modulus of pure titanium caused removal of material and plastic deformation at the thread crests in both groups. Surface changes at the thread crests were evident at 10,000× magnification. Assuming that the maximum stress is applied to the region within which polyurethane deposition was detected, a maximum of 15% of the total implant surface area would be affected.

Similar findings were made by Mints et al.[14], who investigated surface damage at the apical cutting threads. Here, the crest of the inserted implant was smoother than the rougher pristine implant cutting edge. Also Senna et al.[15] described microscopically visible changes like chipping of the porous structures along the surface associated with cracks on the base of the anodized layer.

Laser profilometry enabled more in-depth clarification of the effect of the surgical protocol on the thread flanks. Significant differences in the surface topography were observed in both groups. However, these differences occurred predominantly in the non-threaded group, indicating increased stress to the surface.

The decrease in the core roughness height (S_k), the reduced peak height above the core roughness (S_{pk}), and the reduced valley depth (S_{vk}) led to peak reduction as a result of abrasion, and these results were comparable to those of Senna et al.[15]. Deeper surface profile levels revealed minimal changes, as demonstrated by the stable S_{vk} values. The presence of abrasion was confirmed by the estimated hybrid parameters, which showed a decrease in the extended surface area, S_{3A}, and surface area ratio, S_{dr}.

Due to the in vitro design, this study has some weaknesses, such as the removal of the implants for analysis. As a result, additional damage may have been done to the implant surface. To avoid this, the blocks can be split before implant insertion[14,15]. However, this procedure could change the biomechanical behaviour; therefore this was not done in the present study. As already described by Mints et al.[14] and Senna et al.[15], block residues on the implant surface occurred and the crest threads could not be fully visualized by SEM. Furthermore, only one type of bone density and one type of implant were investigated. However, these factors in particular influence the implant primary stability. Möhlhenrich et al.[32] were able to demonstrate that the primary stability of dental implants increases with increasing density of artificial polyurethane bone blocks, as well as increasing implant diameter and length. Damage to the implant surface may be proportional and this should be the focus of further investigations.

In conclusion, within the limitations of this in vitro investigation, both insertion protocols (non-threaded and threaded) led to significant changes in surface areas, especially at the thread crests in terms of abrasion and deformation. There were also changes in the thread flanks, but these were significantly smaller changes. In particular, the non-threaded protocol led to increased insertion torques, resulting in enhanced stress to the implant surface compared to the threaded protocol. Although the surgical protocol seemed to have a minor influence on surface preservation, further studies analyzing cell activity after damage to the microstructure of dental implant surfaces are necessary.

Acknowledgements. The authors thank Dr Hardt (ZBB, Justus-Liebig-University, Gießen, Germany) for supporting the SEM. We thank Mr Heun (Experimental Laboratory of Prosthetic Dentistry, Justus-Liebig-University, Gießen, Germany), Mr Idel and Mr Brinkmann (Experimental Laboratory, Brassler, Lemgo, Germany) for supporting the image analysis.

Funding. No funding.

Competing interests. BEGO Implant Systems (Bremen, Germany) provided the dental implants needed for this study. Despite this, the authors declare no conflict of interest.

Ethical approval. Not required.

Patient consent. Not required.

References

1. Papaspyridakos P, Chen CJ, Singh M, Weber HP, Gallucci GO. Success criteria in implant dentistry: a systematic review. *J Dent Res* 2012;**91**:242–8.
2. Buser D, Nydegger T, Oxland T, Cochran DL, Schenk RK, Hirt HP, Snetivy D, Nolte LP. Interface shear strength of titanium implants with a sandblasted and acid-etched surface: a biomechanical study in the maxilla of miniature pigs. *J Biomed Mater Res* 1999;**45**:75–83.
3. Piattelli A, Manzon L, Scarano A, Paolantonio M, Piattelli M. Histologic and histomorphometric analysis of the bone response to machined and sandblasted titanium implants: an experimental study in rabbits. *Int J Oral Maxillofac Implants* 1998;**13**:805–10.
4. Cochran DL, Nummikoski PV, Higginbottom FL, Hermann JS, Makins SR, Buser D. Evaluation of an endosseous titanium implant with a sandblasted and acid-etched surface in the canine mandible: radiographic results. *Clin Oral Implants Res* 1996;**7**:240–52.
5. Bryington MS, Hayashi M, Kozai Y, Vandeweghe S, Andersson M, Wennerberg A, Jimbo R. The influence of nano hydroxyapatite coating on osseointegration after extended healing periods. *Dent Mater* 2013;**29**:514–20.
6. Vervaeke S, Collaert B, De Bruyn H. The effect of implant surface modifications on survival and bone loss of immediately loaded implants in the edentulous mandible. *Int J Oral Maxillofac Implants* 2013;**28**:1352–7.
7. Meyer U, Buhner M, Buchter A, Kruse-Losler B, Stamm T, Wiesmann HP. Fast element mapping of titanium wear around implants of different surface structures. *Clin Oral Implants Res* 2006;**17**:206–11.
8. Schliephake H, Reiss G, Urban R, Neukam FW, Guckel S. Metal release from titanium fixtures during placement in the mandible: an experimental study. *Int J Oral Maxillofac Implants* 1993;**8**:502–11.
9. Franchi M, Bacchelli B, Martini D, Pasquale VD, Orsini E, Ottani V, Fini M, Giavaresi G, Giardino R, Ruggeri A. Early detachment of titanium particles from various different surfaces of endosseous dental implants. *Biomaterials* 2004;**25**:2239–46.
10. Franchi M, Orsini E, Martini D, Ottani V, Fini M, Giavaresi G, Giardino R, Ruggeri A. Destination of titanium particles detached from titanium plasma sprayed implants. *Micron* 2007;**38**:618–25.
11. Martini D, Fini M, Franchi M, Pasquale VD, Bacchelli B, Gamberini M, Tinti A, Taddei P, Giavaresi G, Ottani V, Raspanti M, Guizzardi S, Ruggeri A. Detachment of titanium and fluorohydroxyapatite particles in unloaded endosseous implants. *Biomaterials* 2003;**24**:1309–16.
12. Flatebo RS, Hol PJ, Leknes KN, Kosler J, Lie SA, Gjerdet NR. Mapping of titanium particles in peri-implant oral mucosa by laser ablation inductively coupled plasma mass spectrometry and high-resolution optical darkfield microscopy. *J Oral Pathol Med* 2011;**40**:412–20.
13. David G. *Oberflächenbeschaffenheit marktgängiger Implantatsysteme vor und nach der*

knöchernen Insertion. Masterthese. Krems Universität; 2004.
14. Mints D, Elias C, Funkenbusch P, Meirelles L. Integrity of implant surface modifications after insertion. *Int J Oral Maxillofac Implants* 2014;**29**:97–104.
15. Senna P, Antoninha Del Bel Cury A, Kates S, Meirelles L. Surface damage on dental implants with release of loose particles after insertion into bone. *Clin Implant Dent Relat Res* 2015;**17**:681–92.
16. Bartold PM, Kuliwaba JS, Lee V, Shah S, Marino V, Fazzalari NL. Influence of surface roughness and shape on microdamage of the osseous surface adjacent to titanium dental implants. *Clin Oral Implants Res* 2011;**22**:613–8.
17. Irinakis T, Wiebe C. Initial torque stability of a new bone condensing dental implant: a cohort study of 140 consecutively placed implants. *J Oral Implantol* 2009;**35**:277–82.
18. Möhlhenrich SC, Modabber A, Steiner T, Mitchell DA, Hölzle F. Heat generation and drill wear during dental implant site preparation: systematic review. *Br J Oral Maxillofac Surg* 2015;**53**:679–89.
19. de Oliveira PT, Nanci A. Nanotexturing of titanium-based surfaces upregulates expression of bone sialoprotein and osteopontin by cultured osteogenic cells. *Biomaterials* 2004;**25**:403–13.
20. de Oliveira PT, Zalzal SF, Beloti MM, Rosa AL, Nanci A. Enhancement of in vitro osteogenesis on titanium by chemically produced nanotopography. *J Biomed Mater Res A* 2007;**80**:554–64.
21. Svanborg LM, Andersson M, Wennerberg A. Surface characterization of commercial oral implants on the nanometer level. *J Biomed Mater Res B Appl Biomater* 2010;**92**:462–9.
22. Oliveira NT, Guastaldi FP, Perrotti V, Hochuli-Vieira E, Guastaldi AC, Piattelli A, Iezzi G. Biomedical Ti—Mo alloys with surface machined and modified by laser beam: biomechanical, histological, and histometric analysis in rabbits. *Clin Implant Dent Relat Res* 2013;**15**:427–37.
23. Sollazzo V, Pezzetti F, Scarano A, Piattelli A, Bignozzi CA, Massari L, Brunelli G, Carinci F. Zirconium oxide coating improves implant osseointegration in vivo. *Dent Mater* 2008;**24**:357–61.
24. Mohedano M, Matykina E, Arrabal R, Pardo A, Merino MC. Metal release from ceramic coatings for dental implants. *Dent Mater* 2014;**30**:e28–40.
25. Di Iorio D, Traini T, Degidi M, Caputi S, Neugebauer J, Piattelli A. Quantitative evaluation of the fibrin clot extension on different implant surfaces: an in vitro study. *J Biomed Mater Res B Appl Biomater* 2005;**74**:636–42.
26. Rupp F, Scheideler L, Rehbein D, Axmann D, Geis-Gerstorfer J. Roughness induced dynamic changes of wettability of acid etched titanium implant modifications. *Biomaterials* 2004;**25**:1429–38.
27. Sammons RL, Lumbikanonda N, Gross M, Cantzler P. Comparison of osteoblast spreading on microstructured dental implant surfaces and cell behaviour in an explant model of osseointegration. A scanning electron microscopic study. *Clin Oral Implants Res* 2005;**16**:657–66.
28. Nienkemper M, Santel N, Honscheid R, Drescher D. Orthodontic mini-implant stability at different insertion depths: sensitivity of three stability measurement methods. *J Orofac Orthop* 2016;**77**:296–303.
29. Vayron R, Nguyen VH, Lecuelle B, Haiat G. Evaluation of dental implant stability in bone phantoms: comparison between a quantitative ultrasound technique and resonance frequency analysis. *Clin Implant Dent Relat Res* 2018;**20**:470–8.
30. Dos Santos MV, Elias CN, Cavalcanti Lima JH. The effects of superficial roughness and design on the primary stability of dental implants. *Clin Implant Dent Relat Res* 2011;**13**:215–23.
31. Tabassum A, Meijer GJ, Wolke JG, Jansen JA. Influence of surgical technique and surface roughness on the primary stability of an implant in artificial bone with different cortical thickness: a laboratory study. *Clin Oral Implants Res* 2010;**21**:213–20.
32. Möhlhenrich SC, Heussen N, Elvers D, Steiner T, Hölzle F, Modabber A. Compensating for poor primary implant stability in different bone densities by varying implant geometry: a laboratory study. *Int J Oral Maxillofac Surg* 2015;**44**:1514–20.
33. Tabassum A, Meijer GJ, Wolke JG, Jansen JA. Influence of the surgical technique and surface roughness on the primary stability of an implant in artificial bone with a density equivalent to maxillary bone: a laboratory study. *Clin Oral Implants Res* 2009;**20**:327–32.
34. Krafft T, Peschla M. Abrasion of surface components in endosseous implants depending on their shape and coating. *Int J Oral Maxillofac Surg* 1994;**23**:418–9.
35. Palmquist A, Johansson A, Suska F, Branemark R, Thomsen P. Acute inflammatory response to laser-induced micro- and nano-sized titanium surface features. *Clin Implant Dent Relat Res* 2013;**15**:96–104.
36. Wennerberg A, Albrektsson T. Suggested guidelines for the topographic evaluation of implant surfaces. *Int J Oral Maxillofac Implants* 2000;**15**:331–44.

Address:
Stephan Christian Möhlhenrich
Department of Orthodontics and Dentofacial Orthopaedics
RWTH Aachen University Hospital
Pauwelsstraße 30
52074 Aachen
Germany
Tel.: +49 241 8035791
Fax: +49 241 82459
E-mail: smoehlhenrich@ukaachen.de